

Effects of Machine Direction Orientation (MDO) on the Moisture and Oxygen Barrier Properties of HMW-PE Films

D. Ryan Breese
Product Development
Lyondell Chemical Company
11530 Northlake Dr.
Cincinnati, Ohio 45249

Dr. Gregory Beaucage
Department of Chemical and Materials Engineering
University of Cincinnati
Cincinnati, Ohio 45221

KEYWORDS

Moisture, Oxygen, Barrier, MDO, HMW-PE

ABSTRACT

Moisture and oxygen barrier properties of machine direction oriented (MDO) polyethylene films have been studied. This paper will present the effects of density and draw ratio of the MDO film on its barrier properties. This paper will also present the structural changes occurring in the crystalline phase of the MDO film and its relationship with the barrier properties.

INTRODUCTION

Machine direction orientation (MDO) is a process where a film is uniaxially stretched in the machine direction to enhance physical properties. Past work [1] showed significant improvements through MDO processing in the moduli (both machine and transverse directions), yield and break strengths and optical properties (haze & gloss) of polyethylene films. In addition, fiber composite theory can be used to explain the structural changes that occur in the crystalline phase of the polymer [1]. Of additional interest is the effect of the MDO process on the barrier properties of high molecular weight polyethylene (HMW-PE) films. Past work by Duckwall, et al. [2], showed significant improvements in the moisture barrier of HMW-HDPE (high density polyethylene) films after machine direction orientation.

EXPERIMENTAL

Typical high stalk techniques were used to produce a set of 150 μm (six mil) thick films from five HMW-PE polymers. Table 1 lists the densities and MIs for the five grades.

Table 1. Density and MI values for the five HMW-PE grades studied.

	Density (g/cc)	MI (g/10 minutes)
HD 1	0.959	0.057
HD 2	0.949	0.075
HD 3	0.949	0.057
HD 4	0.940	0.10
HD 5	0.938	0.057

The films were produced with a blow up ratio of 3:1 and a stalk height of eight die diameters. The films were then oriented on a Hosokawa-Alpine commercial MDO unit. Each film was drawn to various draw ratios, producing a series of films with various degrees of orientation and final gauges. The draw ratio is defined as the ratio of the undrawn film thickness to the drawn film thickness, as shown in Equation 1.

$$\text{Draw Ratio} = \frac{\text{Undrawn Film Thickness}}{\text{Drawn Film Thickness}} \quad (1)$$

The physical properties of the films were tested and the orientation characterized on various length scales. Through wide angle x-ray scattering (WAXS), small angle x-ray scattering (SAXS), birefringence and Fourier transform-cross polarized optical microscopy techniques, the orientation of the unit cell, lamellae and larger length scale entities were documented and correlated to changes in the structure and physical properties of the film [1].

DISCUSSIONS AND RESULTS

Previous work [1] focused on relating enhancements in moduli, tensile strengths and optical properties to structural changes, but did not expand upon the changes in barrier properties of oriented HMW-PE films. Figure 1 and Figure 2 show that the moisture and oxygen barrier properties improved for the sample with the highest density (HD-1). Such an observation is expected, with the greater amount of the highly ordered crystalline phase restricting the transmission of moisture and oxygen through the sample. As expected, films produced with polymers of lower densities had higher moisture (MVTR) and oxygen (OTR) transmission rates.

Moisture Vapor Transmission Rate of MDO HMW-PE

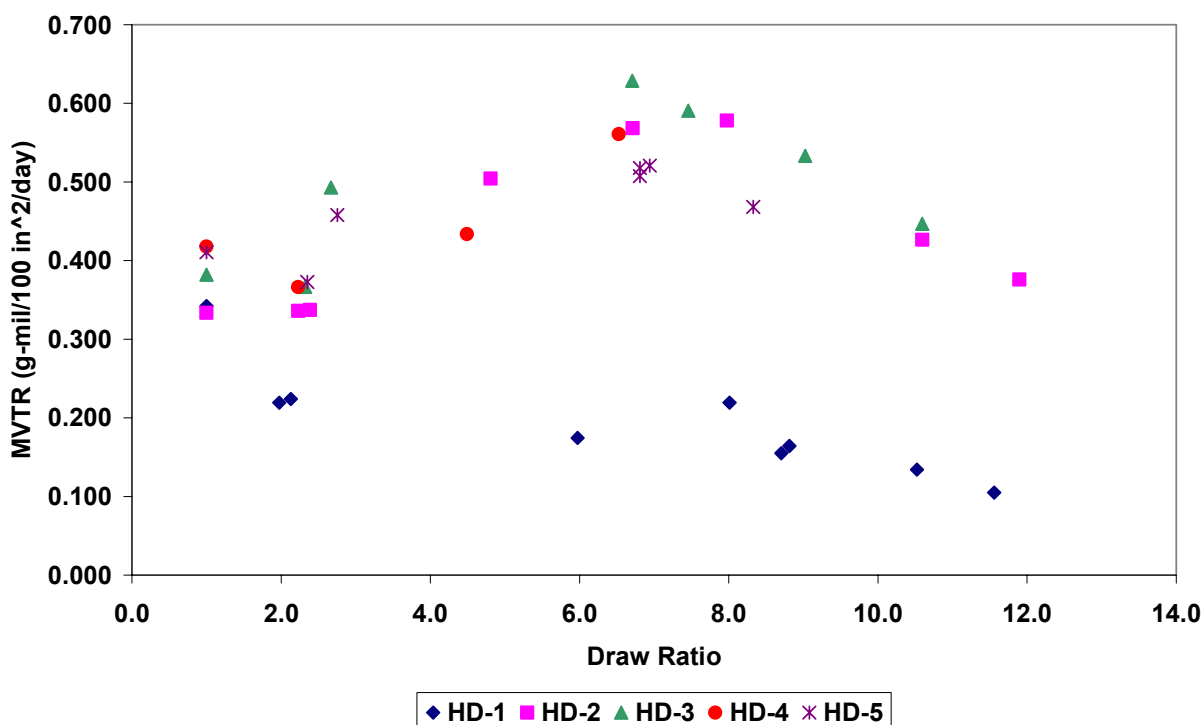


Figure 1. Moisture Vapor Transmission Rate of Drawn HMW-PE Films vs. Draw Ratio. The moisture barrier improves only for the HD-1 when drawn.

Oxygen Transmission Rate of MDO HMW-PE

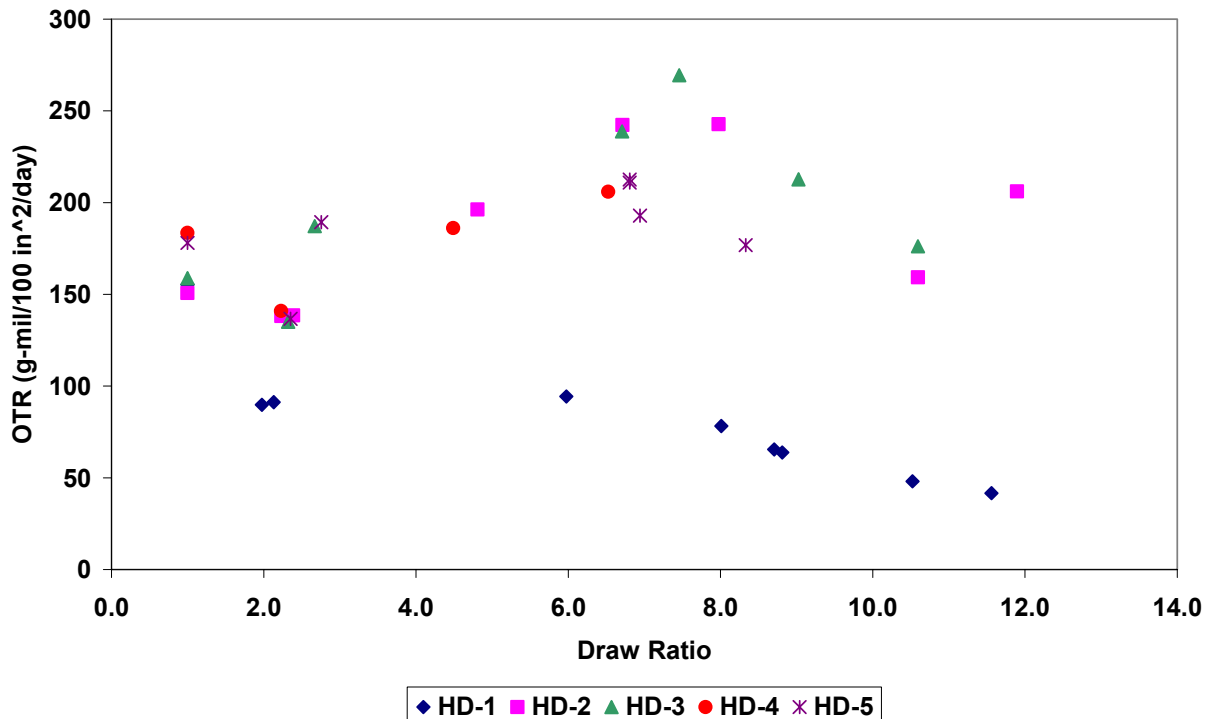


Figure 2. Oxygen Transmission Rate of Drawn HMW-PE Films vs. Draw Ratio. The oxygen barrier improves only for the HD-1 when drawn.

For the lower density samples ($\rho < 0.959$), a peak is evident in both the moisture and oxygen transmission rate data, occurring at a draw ratio of approximately 7:1. This trend is unexpected, based on the work of Duckwall et al. [2]. To explain this phenomena, the barrier data was compared to the structural model described by a collaborative effort [1] to explain how the orientation of the crystalline phase effects the barrier properties of the film.

On a larger length scale, the crystalline lamellae are relatively randomly oriented prior to the MDO process. At low to moderate draw ratios, as shown in Figure 3, the lamellae orient such that their normals align parallel to the machine direction and the c-axis of the unit cell aligns to an angle of $\pm 34.4^\circ$ relative to the lamella normal [3-7]. This is indicated by a Herman's orientation function from SAXS approaching unity and a Herman's orientation function from WAXS approaching 0.521 [1]. At such an arrangement, the lamellae are stacked nearly parallel to each other, exposing inter- and intra- lamellar stack voids that are conducive to the passage of moisture and/or oxygen through the films.

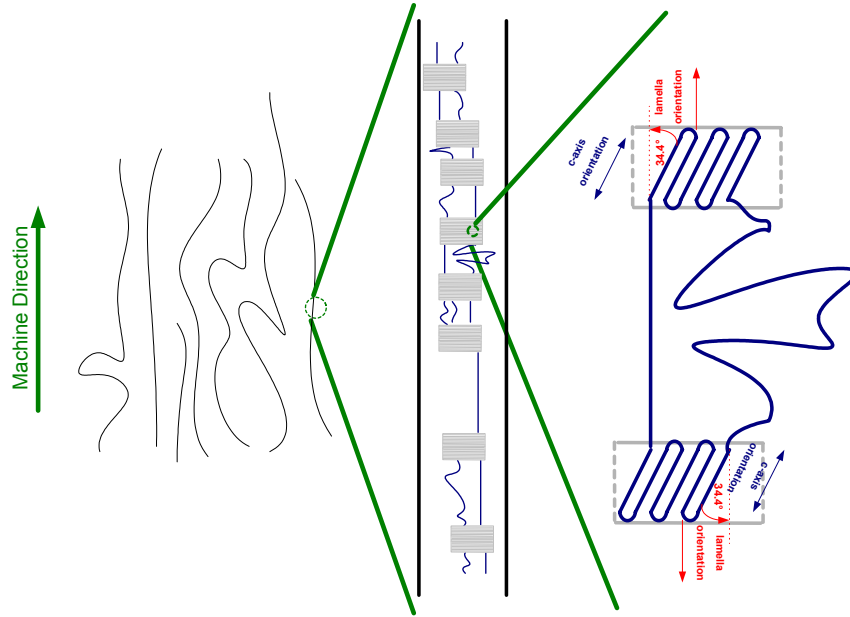


Figure 3. Oriented lamellae clusters and stacks seen at low draw ratios. Lamellae normals are oriented parallel to the drawing direction, the c-axis of the unit cell is oriented at $\pm 34.4^\circ$ relative to the drawing direction.

At higher draw ratios, the orientation process causes the c-axis of the unit cell to align in the drawing direction, as shown in Figure 4, and is indicated by a Herman's orientation function from SAXS approaching 0.521 and a Herman's orientation function from WAXS approaching unity [1]. As a result, the normals of the lamellae are tilted to $\pm 34.4^\circ$ relative to the drawing direction. Such an arrangement forms a more torturous path by blocking the inter- and intra-lamellar stack paths and hindering the transmission of moisture or oxygen through the film sample. This is indicated by a decrease in both the moisture and oxygen transmission rates at draw ratios greater than that required for c-axis alignment in the machine direction.

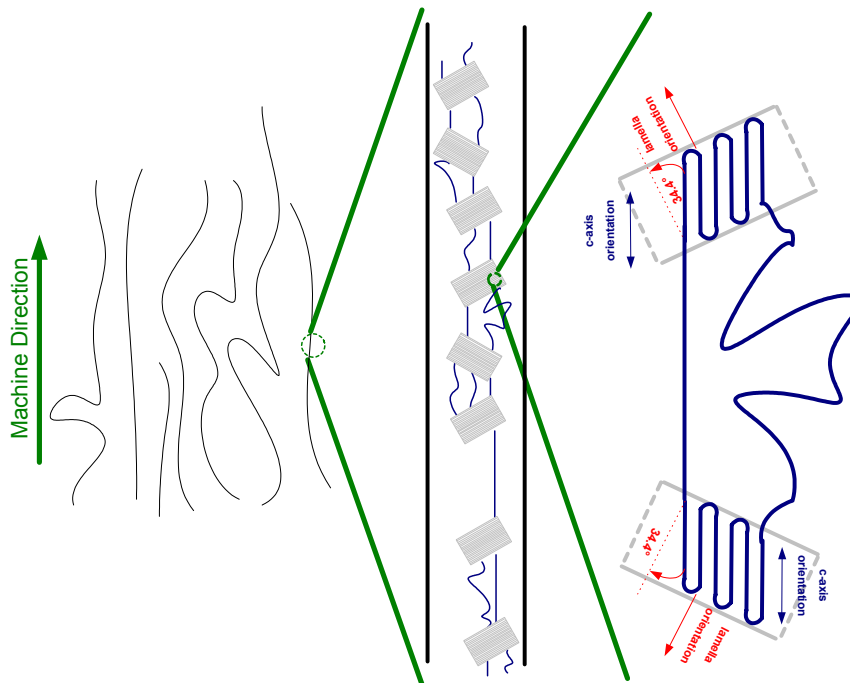


Figure 4. Oriented lamellae clusters and stacks at high draw ratios. Lamellae normals are oriented at $\pm 34.4^\circ$ to the drawing direction, the c-axis of the unit cell is oriented parallel to the drawing direction.

For the (HD-1) sample, a pronounced peak is not observed in either the moisture or oxygen barrier data. This is the result of the lack of film samples available at low draw ratios (between 2:1 and 6:1). In addition, modeling efforts have shown that of all the polymers studied, HD-1 has the greatest tendency to form fibrillar (long-range ordered stacks of lamellae) structures [1], making the window of draw ratios at which the lamellae normals are aligned in the machine direction narrower than other HMW-PEs.

Of all the analytical techniques utilized, the Herman's orientation function determined from birefringence correlated the best with the barrier property changes (Figure 5).

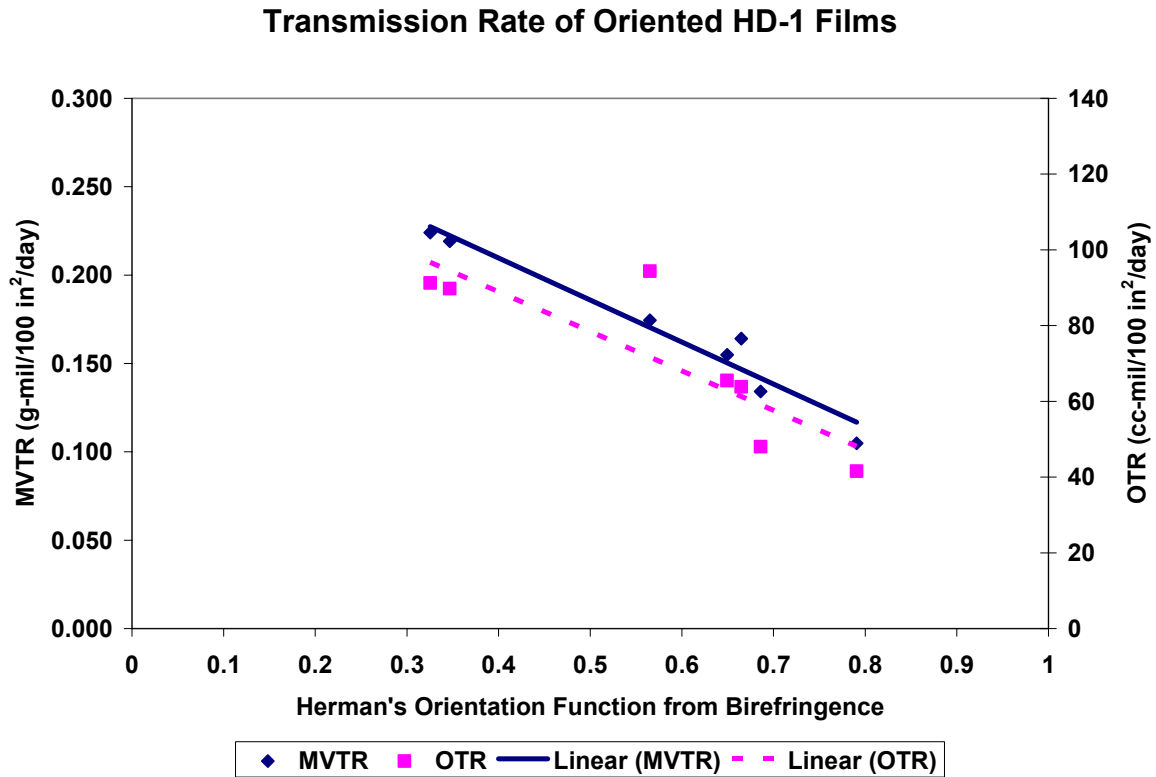


Figure 5. MVTR and OTR data for HD-1 vs. Herman's Orientation Function from Birefringence.

The linear relationship between the barrier data and the Herman's orientation function from birefringence is somewhat expected if one considers the transmission of moisture and oxygen through a polymer in a similar fashion as that of light (birefringence). In essence, this relationship is similar to the stress optical phenomena seen between the birefringence and the stress induced on the polymer. From Figure 5, the relationship between transmission rate and the Herman's orientation function from birefringence ($f_{\text{birefringence}}$) is:

$$\frac{1}{\text{Transmission Rate}} \propto \text{Barrier Property} \propto f_{\text{birefringence}} \quad (2)$$

The birefringence (Δn) and the Herman's orientation function are related by Equation (3), where Δn_o is the intrinsic birefringence that is characteristic of a given material [8].

$$\Delta n = \Delta n_o * f_{\text{birefringence}} \quad (3)$$

The Herman's orientation function measured from birefringence is linearly proportional to the draw ratio of the film, as indicated in Figure 6, resulting in Equation 4.

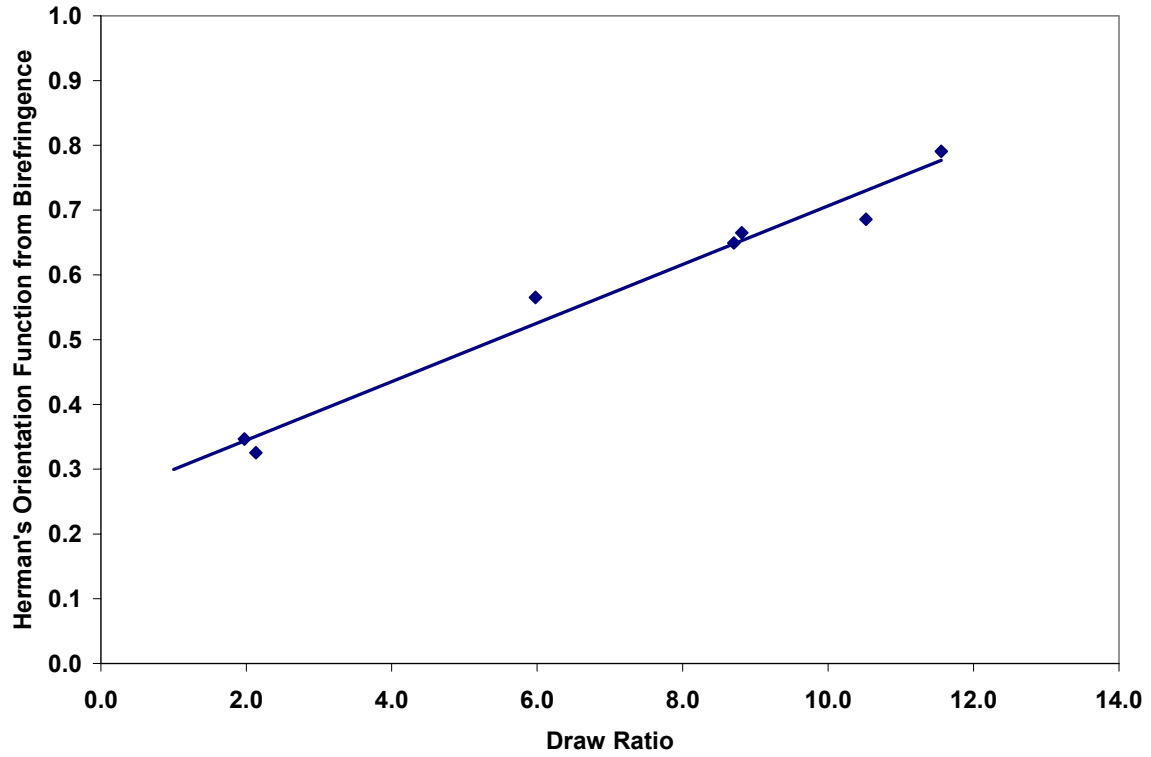


Figure 6. Plot of Herman's Orientation Function from Birefringence vs. Draw Ratio.

$$f_{birefringence} \propto Draw Ratio \quad (4)$$

The stress optical law [9] states that the birefringence (Δn) is proportional to the tensile stress (σ_{zz}) that is applied to the system at low to moderate tensile stresses, resulting in the following equation, where $C_{optical}$ is a constant that is specific to a given material [10].

$$\Delta n \approx C_{optical} * \sigma_{zz} \quad (5)$$

Combining Equations (3), (4) and (5) shows that the draw ratio is proportional to the stress induced in the machine direction (σ_{zz}).

$$Draw Ratio \propto \sigma_{zz} \quad (6)$$

Relating the changes in optical anisotropy to that of barrier and utilizing Equations (4), (5) and (6), we obtain:

$$Barrier Property \propto C_{barrier} * (f_{birefringence}) \quad (7)$$

$C_{barrier}$ is an orientation-barrier coefficient and refers to the slope of the linear regression of the barrier data and the Herman's orientation function from birefringence and is indicative of the change in transmission rate through the given material with respect to degree of orientation measured from birefringence.

It is interesting to see that the barrier data correlates well with the orientation calculations from birefringence and not those calculated from SAXS, WAXS or Fourier transform-cross polarized optical microscopy techniques (located in the Appendix). This indicates that, since the birefringence techniques includes contributions from both the amorphous and crystalline phases while the other techniques only characterize the crystalline phase, changes in the amorphous phase plays a role in the barrier properties of the polymer. Future work will be conducted using infrared dichroism, since this technique can characterize both amorphous, crystalline and a combination of both phases [11, 12]. This work will provide a better understanding of how the orientation of the amorphous and crystalline phases in high density polymers affects barrier properties.

CONCLUSIONS

A significant decrease in both moisture and oxygen transmission rates is observed with the machine direction orientation of homopolymer HMW-PE films. Intermediate and lower density polymers do not show such a significant decrease, and actually present a maximum at moderate draw ratios where the transmission rate is greater after orientation than that of the undrawn sample. This maximum is likely resulted from the high degree alignment of the lamellar normals in the machine direction, which opens inter- and intra- lamella stack voids for the transmission of both moisture and oxygen. At higher draw ratios, the lamella tilt to $\pm 34.4^\circ$ of the machine direction, making a crossing pattern that blocks the voids of the lamellae. In addition, a linear relationship was observed between the moisture and oxygen transmission rates and the Herman's orientation functions calculated from birefringence, indicating a relationship between the barrier and the degree of orientation similar to that of the stress optical law. The good correlation with birefringence orientation data and weaker correlation with crystallographic techniques indicate that changes in both the amorphous and crystalline regions affect the barrier properties of the sample. Future work could be conducted with an additional technique that accounts for the orientation of both crystalline and amorphous phases, such as IR dichroism, to further understand each phase's effect on barrier.

ACKNOWLEDGEMENTS

The authors would like to thank Equistar Chemicals, a Lyondell Company, for the polymer samples, and for access to the blown film equipment, and Hosokawa-Alpine for access to their MDO unit. We would also like to acknowledge Drs. Doug McFaddin, Ayush Bafna and Fran Mirabella for their assistance with the interpretation of the changes in the crystalline structure.

REFERENCES

1. Breese, D. R., MS Thesis, University of Cincinnati (2005).
2. Duckwall, L. R., Bastian, D. H., Hatfield, E., US Patent # 6,391,411 (2002).
3. Bassett, D. C., Olley, R. H., Al Raheil, I. A. M., *Polymer*, 29, 1539, (1988).
4. Hosier, I. L., Bassett, D. C., Moneva, I. T., *Polymer*, 36, 4197, (1995).
5. Abo el Maaty, M. I., Bassett, D. C., *Polymer*, 42, 4957, (2001).
6. Patel, D., Bassett, D. C., *Polymer*, 43, 3795, (2002).
7. Abo el Maaty, M. I., Bassett, D. C., *Journal of Macromolecular Science: Part B-Physics*, B42, 687, (2003).
8. Campbell, D., Pethrick, R. A., White, J. R., *Polymer Characterization, Physical Techniques*, Stanley Thornes (Publishers) Ltd., 2000.
9. Doi, M., *Introduction to Polymer Physics*, Oxford University Press (1996).
10. Strobl, G., *The Physics of Polymers*, Springer (1996).
11. Koenig, J. L., Cornell, S. W., Witenhafer, D. E., *Journal of Polymer Science: Part A-2*, 5, 301, (1967).
12. Read, B. E., Stein, R. S., *Macromolecules*, 1 (2) 116 (1968).

APPENDIX

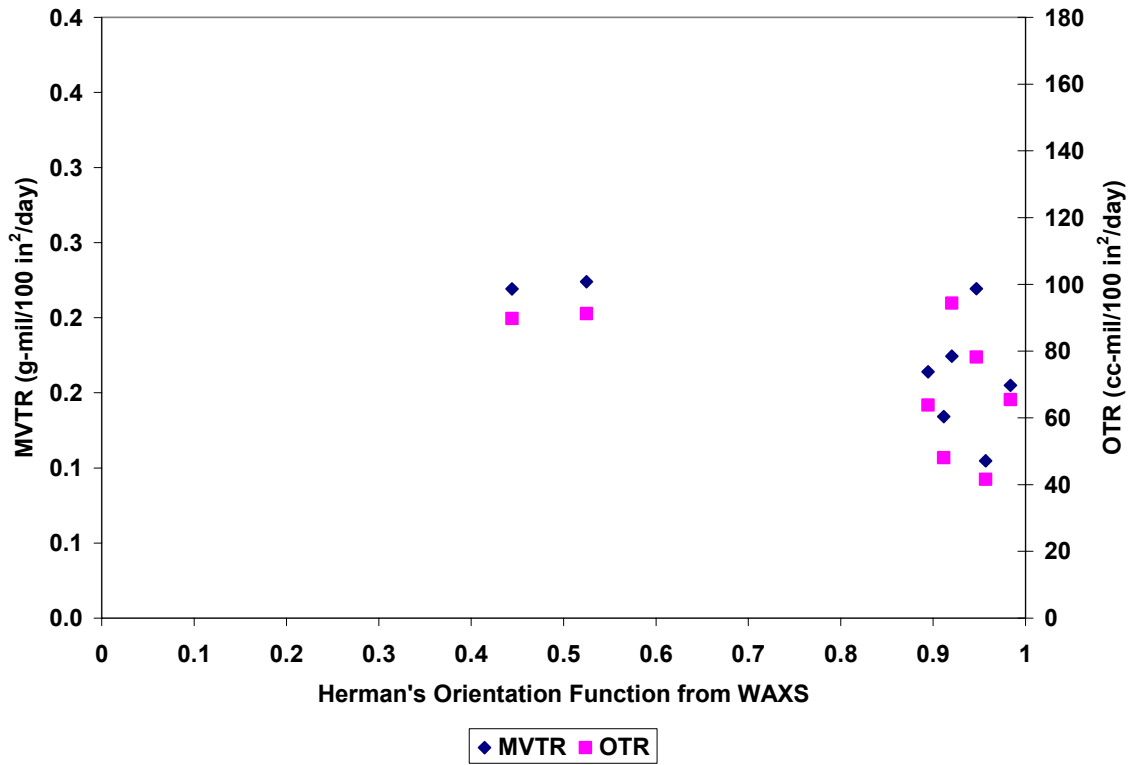


Figure 7. MVTR and OTR Data for HD-1 vs. Herman's Orientation Function from WAXS.

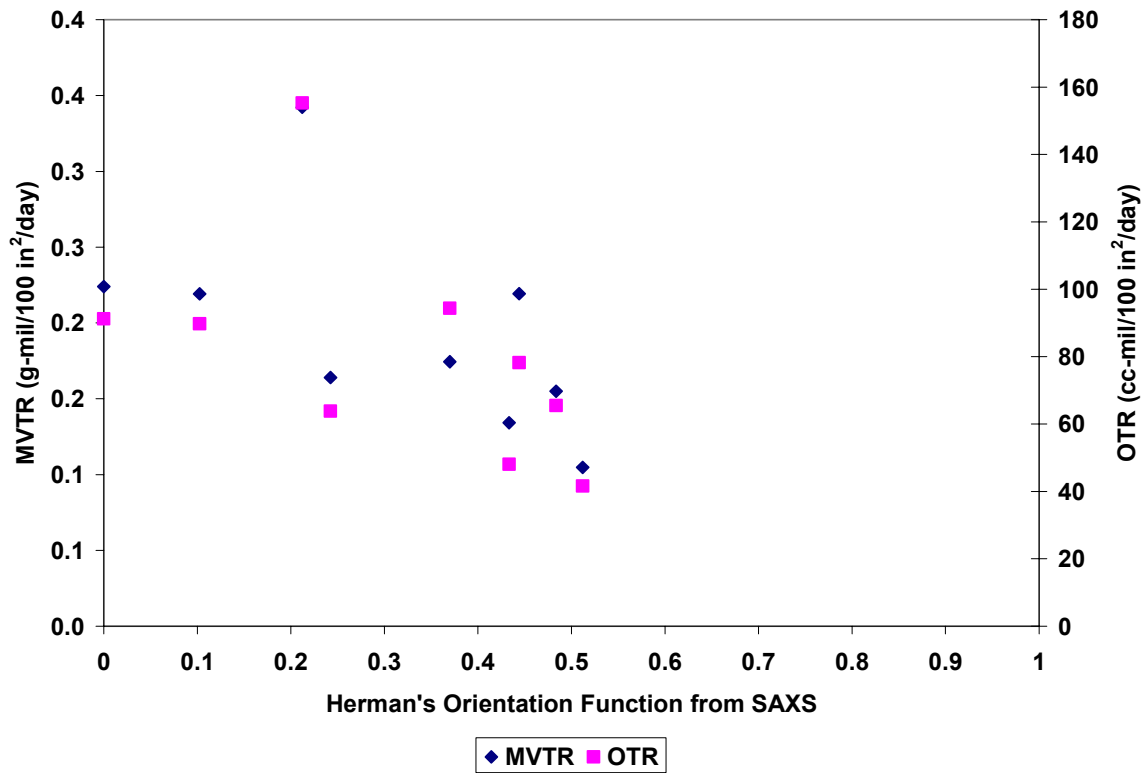


Figure 8. MVTR and OTR Data for HD-1 vs. Herman's Orientation Function from SAXS.

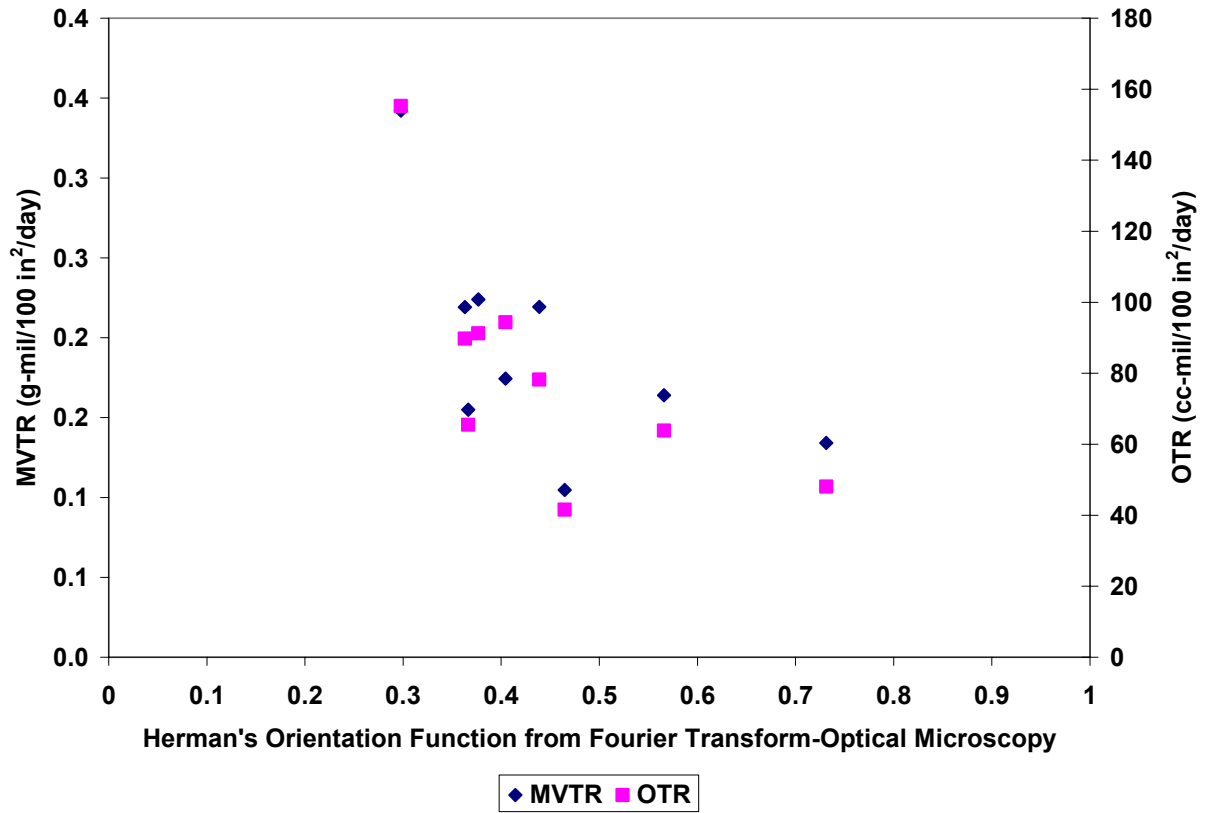


Figure 9. MVTR and OTR Data for HD-1 vs. Herman's Orientation Function from Fourier Transform-Cross Polarized Optical Microscopy.